Molecular Therapy
Nucleic Acids
Original Article

The Identification of Long Non-coding RNA H19 Target and Its Function in Chronic Myeloid Leukemia

Juhua Yang,[1,2,3,6] Zhao Yin,[1,2,3,4,6] Yumin Li,[5,6] Yanjun Liu,[1,2,3] Guiping Huang,[1,2,3] Chunming Gu,[1,2,3,4] and Jia Fei[1,2,3,4]

[1]Department of Biochemistry and Molecular Biology, Medical College of Jinan University, Guangzhou 510632, China; [2]Engineering Technology Research Center of Drug Development for Small Nucleic Acid, Guangdong Province, China; [3]Antisense Biopharmaceutical Technology Co., Ltd., Guangzhou, China; [4]Insititute of Chinese Integrative Medicine, Medical College of Jinan University, Guangzhou 510632, China; [5]Medical Laboratory of Shenzhen Luohu People's Hospital, Shenzhen, China

H19 is a long non-coding RNA which was lowly expressed in chronic myeloid leukemia (CML). Here, we found that the overexpression of H19 significantly inhibited cell viability and colony formation and prolongs survival in CML cell lines and three xenografted mouse models. The H19 target proteins and microRNAs (miRNAs) were identified using a combination of computational prediction and RNA pull-down, including PCBP1, FUS protein, and miR-19a-3p and miR-106b-5p. Targeting PCBP1, FUS protein, miR-19a-3p, and miR-106b-5p significantly inhibits the cell growth and colony formation of CML cell lines. Co-overexpression of H19 and PCBP1, FUS, miR-19a-3p, and miR-106b-5p decreases the inhibitory effect of H19 in CML. These findings might provide a novel molecular insight into CML.

INTRODUCTION

Chronic myeloid leukemia (CML) is a clonal myeloproliferative disorder of the hematopoietic stem cells caused by abnormal tyrosine kinase activity of the breakpoint cluster region protein (BCR)/Abelson murine leukemia viral oncogene homolog (ABL) (BCR-ABL) translocation, which was generated from a reciprocal translocation between chromosomes 9 and 22, known as the Philadelphia (Ph) chromosome.[1] CML affects about one individual per 100,000 per year and makes up for 15% of all new cases of leukemia in the Western hemisphere.[2] On the basis of the process of disease, CML is clinically divided into three stages: the chronic phase (CP), then an accelerated phase (AP), and a terminal blast crisis (BC).[1]

Long non-coding RNAs (lncRNAs), imperative non-coding RNAs, consist of at least 200 nucleotides and are characterized by a lack of protein-coding capacity.[3,4] lncRNAs are involved in numerous biological processes and regulatory mechanisms including DNA damage, angiogenesis, microRNA silencing, invasion and metastasis, and programmed cell death.[5] Moreover, lncRNAs can also regulate embryonic development, inflammation, immune cell development, and tumor development.[6–8] lncRNAs are closely linked with several regulatory mechanisms, including cell cycle control, gene imprinting, mRNA degradation, splicing regulation, chromatin remodeling, translocational regulation, and epigenetic regulation.[5]

The H19 gene is a highly conserved and maternally expressed imprinted gene located on human chromosome 11p15.5. It encodes a non-coding RNA that is 2.3 kb in size and plays an imperative role in mammalian and embryonal development.[9–12] Furthermore, recent studies have shown that H19 is closely associated with cell proliferation and metastasis in a variety of cancers, such as bladder cancer,[13] colorectal cancer,[14] gastric cancer,[15] esophageal cancer,[16] and so on. Although H19 has been shown to play a key role in multiple cancers and it has been reported that hypomethylation-mediated H19 overexpression increases the risk of CML,[17] the specific mechanism of H19 in CML remains to be elucidated. Thus, we researched the role of H19 in CML and it's targeted proteins and microRNAs (miRNAs).

miRNAs are non-coding single-strand RNAs consisting of approximately 22 nucleotides in length.[18] These miRNAs regulate the expression of protein-coding genes by binding with the 3′ UTRs (3′ untranslated regions) of the targeted mRNAs. A majority of miRNAs share only partial complementarity with their mRNA targets, nevertheless 7–8 nt in the 5′ end of miRNAs, known as the seed sequence, bind to the mRNA in fact.[19] In our study, we used locked nucleic acids' (LNAs') modified seed sequences to knockdown miRNA.

RESULTS

Overexpressing H19 Inhibits the Proliferation of K562 Cells and Prolongs the Survival of the CML Model Mouse

The relative mRNA expression of H19 in K562 cells and normal samples was measured by real-time PCR. The results revealed that the relative mRNA expression of H19 was significantly lower in K562 cells than in normal samples (Figure 1A). To test the role of H19 in CML, we constructed the K562 cells overexpressing H19 by transfecting the K562

Received 7 June 2019; accepted 14 January 2020;
https://doi.org/10.1016/j.omtn.2020.01.021.

[6]These authors contributed equally to this work.

Correspondence: Jia Fei, Department of Biochemistry and Molecular Biology, Medical College of Jinan University, 601 Western Huangpu Avenue, Guangzhou 510632, China.
E-mail: tfeijia@jnu.edu.cn

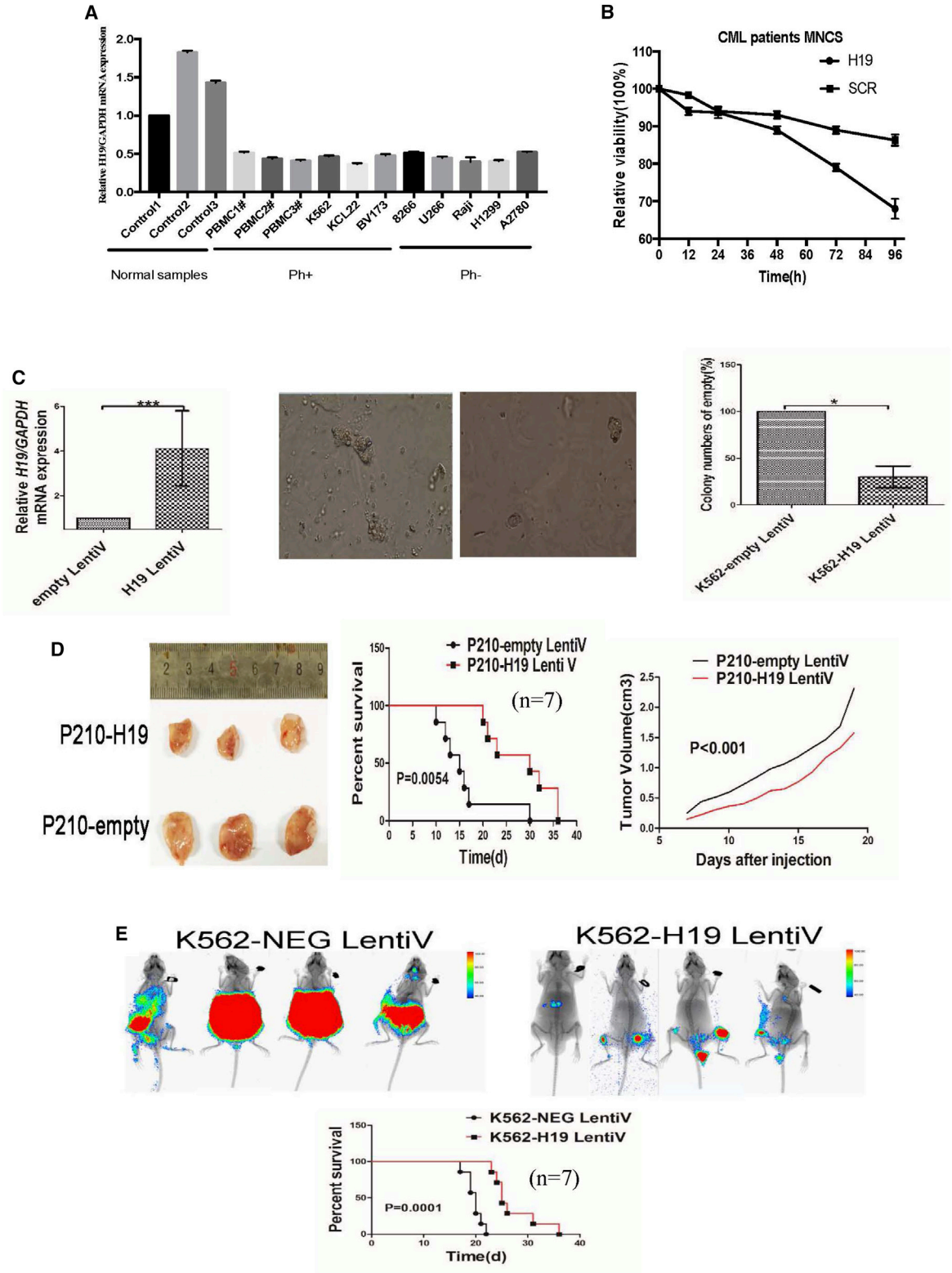

(legend on next page)

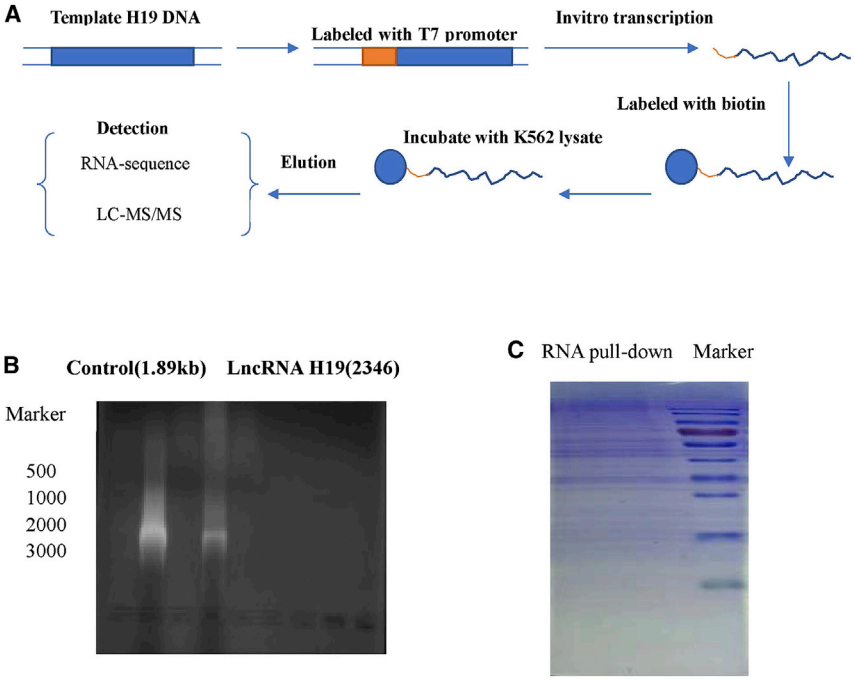

Figure 2. lncRNA H19 Was Obtained by *In Vitro* Transcription, and RNA-Protein-Binding Compounds Were Produced by RNA Pull-Down

(A) The proposed model of *in vitro* transcription and RNA pull-down assay. (B) The DNA template with T7 promoter upstream of the sequence was transcribed into lncRNA H19 *in vitro*. The lncRNA H19 was validated by agarose gel electrophoresis. (C) Cell lysis buffer from K562 were used for the RNA pull-down assay. The binding proteins were separated by 10% SDS-PAGE, visualized by Coomassie blue staining.

cells with the H19-expressing vector and selecting positive cells using puromycin. CML patients' bone marrow mononuclear cells were overexpressed with H19 lentivirus. Colony-forming assays were performed to measure the colony-forming ability of K562 cells. Overexpression of H19 in CML patients' bone marrow mononuclear cells significantly inhibited the cell growth (Figure 1B). As shown in Figure 1C, overexpressing of H19 significantly decreased the number of colonies in K562 cells transfected with H19, compared to the empty vector transfection. The results indicate that overexpression of H19 significantly decreased the colony-forming ability in K562 cells. The tumor size and tumor volume were recorded of each group and the overall survival was monitored by Kaplan-Meier analysis. The results showed that overexpression of H19 prolonged the overall survival of recipient mice (Figures 1D and 1E).

lncRNA H19 Was Obtained by *In Vitro* Transcription, and RNA Protein-Binding Compounds Were Produced by RNA Pull-Down

To identify the molecular mechanism and binding partners of lncRNA H19 in K562 cells, the DNA template with T7 promoter was transcribed into lncRNA H19 that was verified by agarose gel electrophoresis (Figure 2B). Biotinylated lncRNA H19 was mixed with cell lysis buffer followed by incubation with washed streptavidin magnetic beads. Then the complexes were eluted and lncRNA H19 protein-binding compounds were separated by 10% SDS-PAGE, concretized by Coomassie blue staining (Figure 2C).

Identification of the Targets of lncRNA H19

To identify the targeted proteins and miRNAs of lncRNA H19, we performed mass spectrometry and RNA sequencing (RNA-seq) followed by RNA pull-down assay. The catRAPID and starBase v. 2.0 predicted the targeted proteins of lncRNA H19. PCBP1 and FUS protein prediction can be detected by mass spectrometry (MS) (Figure 3A). Then PCBP1 and FUS from RNA pull-down products were tested by western blot (Figure 3B). There are five targeted miRNAs of lncRNA H19 predicted by the starBase v 2.0 (Figure 3C). The five miRNAs can also be monitored by RNA-seq. Two miRNAs of miR-19a-3p and miR-106b-5p are confirmed by real-time PCR (Figure 3D).

The Targeted Inhibition of PCBP1, FUS, miR-19a-3p, and miR-106b-5p Could Reduce the Malignant Progression of K562 Cells

Next, we studied whether inhibiting PCPB1 and FUS by PCBP1 (small interfering RNA) siRNA and FUS siRNA could attenuate CML malignant behavior. As indicted in Figure 4A, either PCPB1 siRNA or FUS siRNA increased K562 cell sensitivity on imatinib (IM) treatment; PCPB1 siRNA or FUS siRNA inhibited the cell growth of CML patients' bone marrow mononuclear cell (MNCs). Colony-formation assay revealed that the colony-forming ability of

Figure 1. H19 Inhibits the Proliferation of K562 Cells and Extend the Survival of the CML Model Mouse

(A) The mRNA expression level of H19 was measured using real-time PCR in normal samples group, CML cell lines, and primary CML cells. The mRNA expression level of H19 was moderately lower in K562 KCL-22 and BV173 cells compared with normal control. (B) CML patient bone marrow mononuclear cells were constructed by transfecting with H19 lentivirus, and the viability of cells was determined by MTT assay. (C) K562 cells overexpressing H19 were constructed by transfecting with H19 plasmid. The mRNA expression level of H19 in K562-H19 LentiV and K562 empty LentiV cells were measured using real-time PCR (***$p < 0.001$, K562-H19 LentiV group versus K562 empty LentiV group). (C) Colony-formation assays. A total of 1,000 cells transfected with empty or H19 plasmids were mixed with RPMI-1640 medium containing 0.9% methylcellulose solution and 20% FBS and then seeded into 24-well plates. Colony numbers were counted 1 week later (*$p < 0.05$, K562-H19 group Lenti versus K562-empty LentiV group). (D) Influence of overexpression of H19 on xenograft models of BaF3-P210 cells. The tumor size after the injection with P210-H19 and P210-empty cells (left); the survival analysis of CML BALB/c nude mice (n = 7) treated with P210-H19 and P210-empty cells (middle); the tumor volume of BALB/c nude mice days after injection (right). (E) NOD/SCID mice (n = 7) were transplanted with the K562 cells overexpressing H19 and K562 cells of negative control. The incidence and survivals of mice after cell injection was shown by the *in vivo* imaging systems.

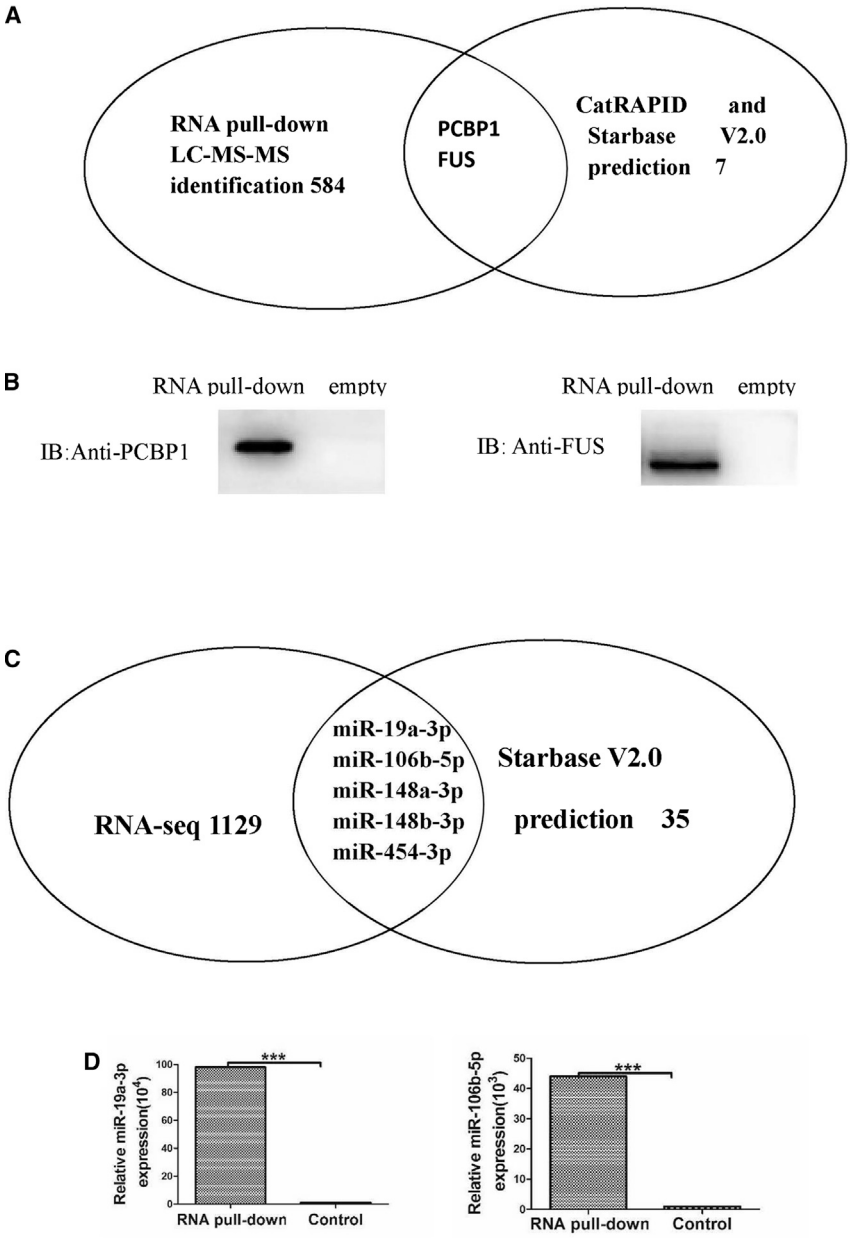

Figure 3. lncRNA H19 Could Target PCBP1 and FUS Protein and Could Target miR-19a-3p and miR-106b-5p in CML

(A) PCBP1 and FUS proteins have been found in the mass spectra results of long non-coding RNA H19 pull-down products. catRAPID and starBase v. 2.0 predicted that PCBP1 and FUS are the interactive proteins of the long non-coding RNA H19. (B) The products of RNA pull-down were detected by immunoblotting using rabbit anti-PCBP1 antibody and using rabbit anti-FUS antibody. (C) lncRNA H19 targets were identified by combining starBase v. 2.0 prediction and RNA-seq results of lncRNA H19 pull-down products. The hsa-miR-19a-3p, hsa-miR-106b-5p, hsa-miR-148a-3p, hsa-miR-148b-3p, and hsa-miR-454-3p identified by both methods were considered as candidate targets of lncRNA H19. (D) The identification of miR-19a-3p and miR-106b-5p by real-time PCR.

K562 cells transfected with PCPB1 and FUS siRNA was significantly reduced compared to cells transfected with Scramble RNA (SCR) ($p < 0.01$) (Figure 4B). Coexpression of H19 and FUS or PCPB1 plasmid in K562 cells reverses the inhibitory effects of H19 (Figures 4C and 4D). Taken all together, these statistics demonstrate that targeted inhibition of PCPB1 and FUS attenuate CML malignant proliferation.

The Targeted Inhibition of miR-19a-3p and miR-106b-5p Could Decrease the Malignant Progression of K562 Cells

To confirm the effect of miR-19a-3p and miR-106b-5p on cell viability, the t-anti-miR-19a-3p and t-anti-miR-106b-5p were transfected into K562 cells for 48 h, and the cell viability and colony-formation assay were performed. As shown in Figure 5A, the t-anti-miR-19a-3p and t-anti-miR-106b-5p can significantly reduce cell viability with SCR controls. The colony-forming capability of K562 cells transfected with t-anti-miR-19a-3p and t-anti-miR-106b-5p was notably reduced compared to cells transfected with SCR (Figure 5B). Coexpression of H19 and miR-19a-3p or miR-106b-5p mimics in K562 cells reverse the inhibition of cell growth of H19 (Figures 5C and 5D). Taken all together, these statistics demonstrate that H19 sponges miR-19a-3p and miR-106b-5p attenuate CML malignant proliferation.

Overexpressing H19 Expands the Survival of Patient-Derived Xenografts in the CML Model Mouse

To identify the effect of overexpression of H19 in patient-derived xenografts in a CML model mouse, we constructed the H19 lentiviral transduction in CML patients, bone marrow cells. As shown in Figure 6, these results showed that overexpression of H19 prolonged the overall survival of recipient mice (Figures 6A and 6B).

DISCUSSION

Studies have shown that H19 differentially methylated region/imprinting control region (DMR/ICR) was hypomethylated and associated with H19 expression in CML patients. Furthermore, demethylation of H19 DMR/ICR reactivated H19 expression in K562 cells.[17] A reduction of H19 expression was observed in all leukemia samples, including chronic myelomonocytic leukemia (CMML; n = 43), CML (n = 40), and acute myelogenous leukemia (AML; n = 32) cases

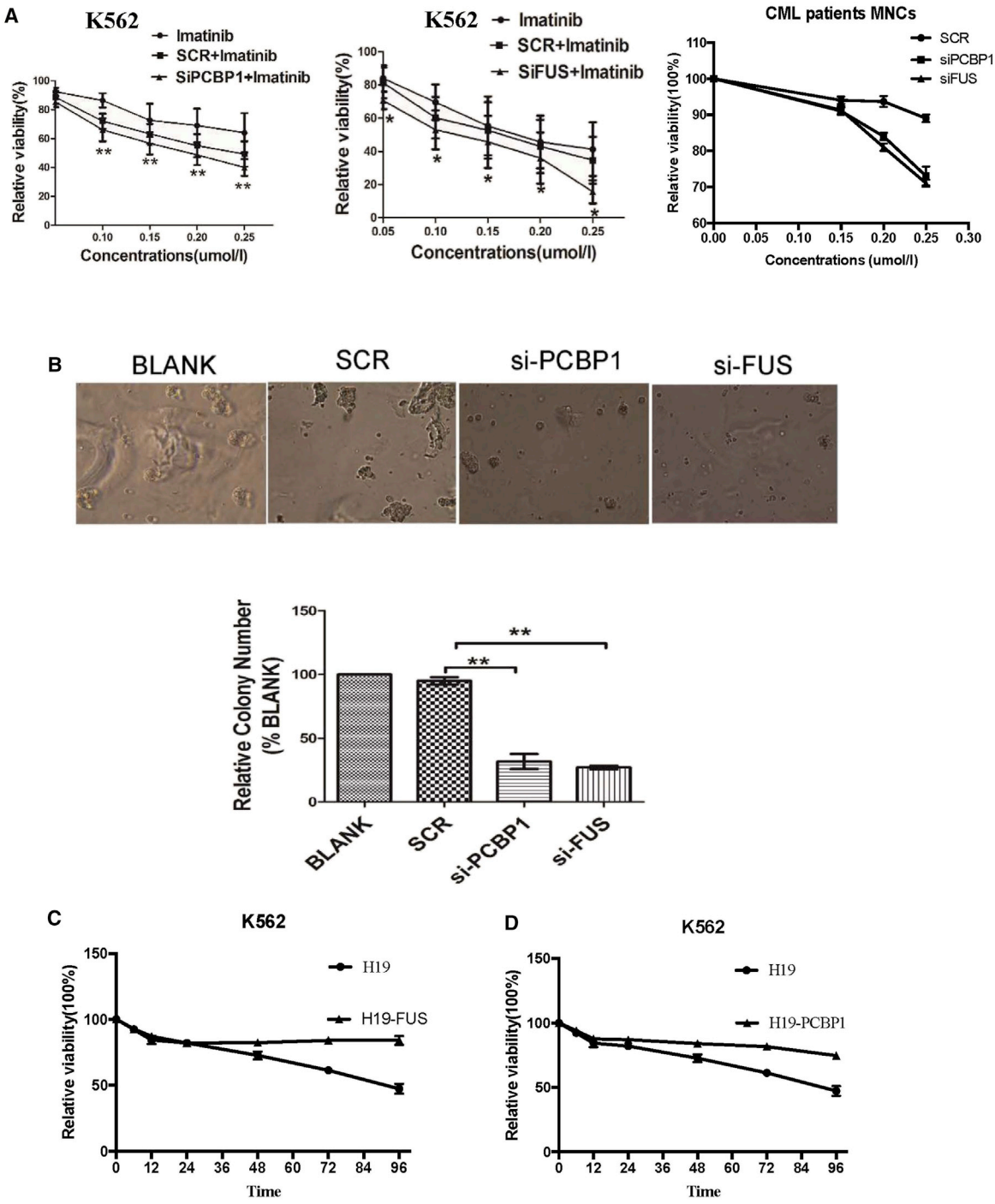

Figure 4. The Targeted Inhibition of PCBP1 and FUS Could Reduce the Malignant Progression of CML Cells

(A) K562 cells and CML patient bone marrow mononuclear cells transfected with SCR, PCBP1 siRNA, and FUS siRNA were treated with different concentrations of imatinib (0–0.25 μM) for 48 h, and the viability of cells was determined by MTT assay (**$p < 0.01$, *$p < 0.05$, PCPB1-siRNA and FUS-siRNA transfected groups versus K562 group and SCR transfected group). (B) Inhibition of PCPB1 and FUS reduces colony formation of K562 cells. A total of 1,000 K562 cells transfected with SCR, PCBP1, and FUS were mixed with RPMI-1640 medium containing 0.9% methylcellulose solution and 20% FBS and seeded into 24-well plates. Colony numbers were counted after 1 week. Histogram and statistics indicating the relative number of colonies per 1,000 plated cells are shown. Statistical significance was assessed by one-way ANOVA (**$p < 0.01$). (C) K562 cells were co-transfected with H19 lentivirus and FUS plasmid, and the viability of cells was determined by MTT assay. (D) K562 cells were co-transfected with H19 lentivirus and PCBP1 plasmid, and the viability of cells was determined by MTT assay.

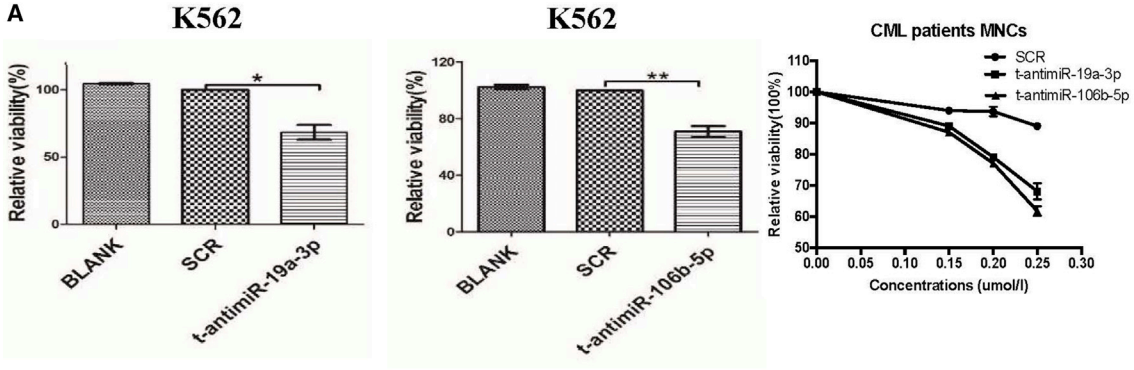

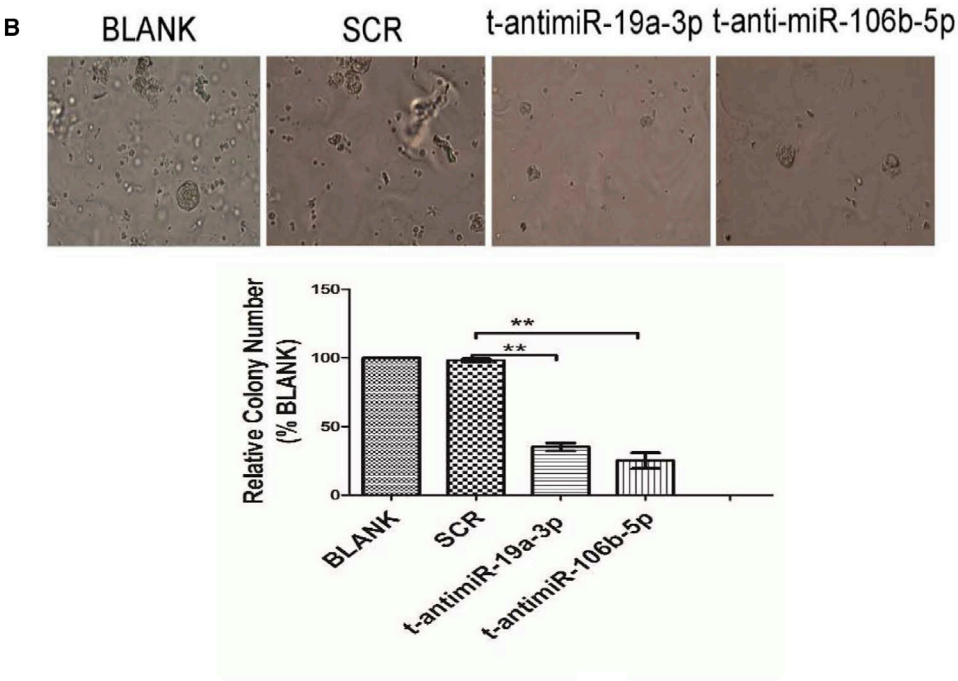

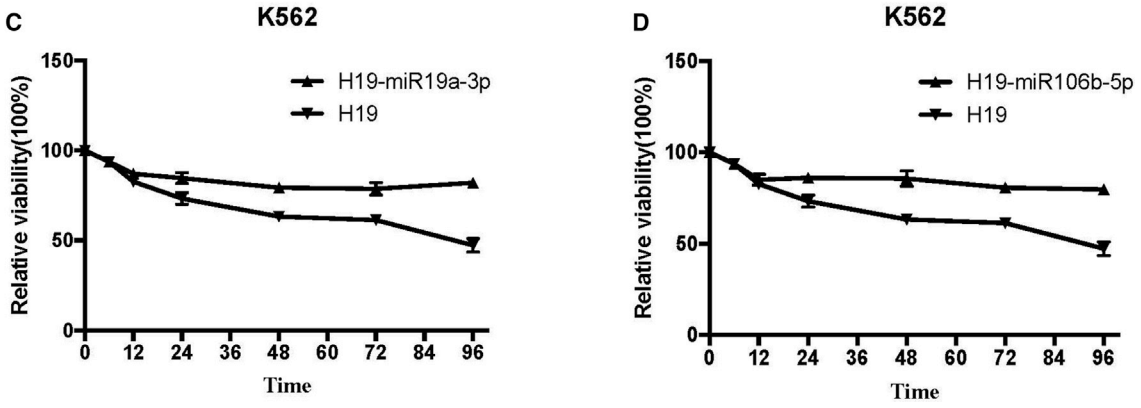

(legend on next page)

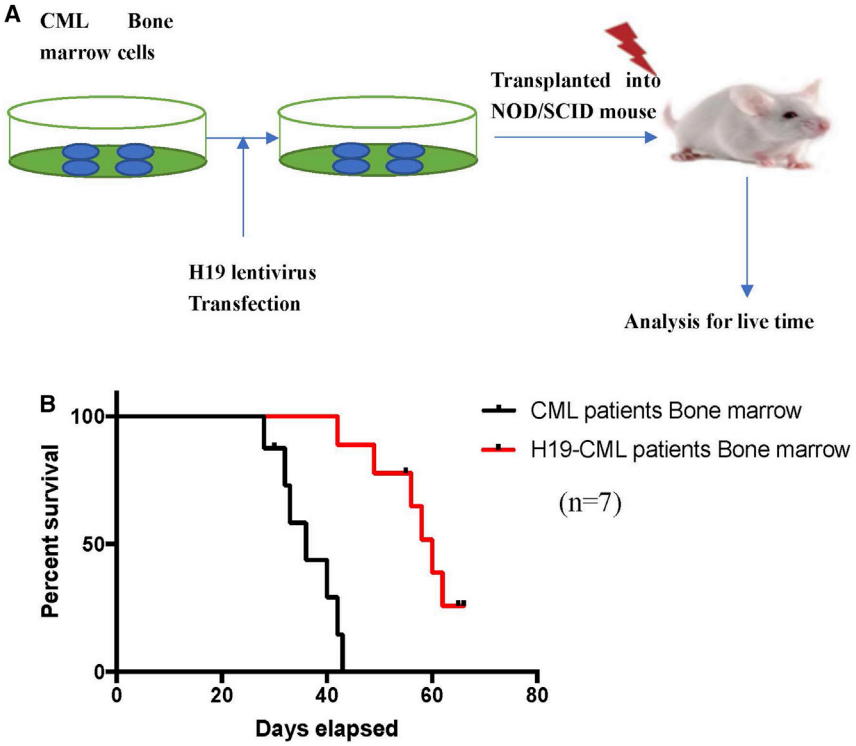

Figure 6. Influence of Overexpression of H19 on Patient-Derived Xenograft Models

(A) Schematic diagram of patient-driven CML mouse model and H19 treatment. (B) Kaplan–Meier survival curves of mice treated with H19, The results showed that overexpression of H19 prolonged the overall survival of recipient mice (n = 7).

compared to the healthy controls including peripheral blood samples from normal (n = 98).[20] H19 was initially identified as a tumor suppressor. Indeed, its overexpression in some tumor cells was associated with inhibition of proliferation, morphological changes, decrease of clonogenicity in soft agar, and tumorigenicity in nude mice.[21] In our study, the expression of H19 was tested in blood samples from normal people (n = 4), in CML patients' peripheral blood mononuclear cells (n = 3), K562 cells, KCL-22 cells, BV173 cells, 8266 cells, U266 cells, Raji cells, H1299 cells, and A2780 cells. A decrease of H19 expression was viewed in all cancer cells compared to the healthy controls (Figure 1A), but another research has the different results it need further detection.[22] Next, we studied the effect of H19 overexpression on K562 cells and CML patients' bone mononuclear cells by colony-formation assays and 3-(4, 5-dimenthyl-thiazol-2-yl)-2, 4-diphenyl-tetrazolium bromide (MTT) assays. The results show that overexpression of H19 inhibited the cell growth of CML patients' bone mononuclear cells and inhibited the colony-formation ability of K562 cells (Figures 1B and 1C). To further research the effect of H19 on a xenograft mouse model of human CML, the P210 cells and K562 cells overexpressing H19 were constructed. The P210 cells transfected with H19 or empty vector were injected into sublethally irradiated (3 Gy) BALB/c recipient mice subcutaneously and the H19 transfected K562 cells were injected into 5-week-old, sublethally irradiated (3 Gy) NOD/SCID recipient mice randomly via tail vein. The survival of the xenograft mouse model of human CML was observed, and the overall survival was prolonged (Figures 1D and 1E).

To elucidate the molecular mechanism of H19 in CML, the targeted proteins and miRNAs were identified by performing MS and RNA-seq followed by RNA pull-down. 586 proteins were detected by MS from RNA pull-down products. Two proteins predicted by catRAPID and starBase v2.0 also existed in MS. Thus, we take the PCPB1 and FUS proteins as the candidates of lncRNA H19 (Figure 3A). PCBP1 and FUS proteins can be detected by immunoblotting in RNA pull-down products (Figure 3B). 1,129 small RNA were detected by RNA-seq from RNA pull-down products, and 35 miRNAs were predicted by starBase v. 2.0. Five miRNAs existed not only in RNA-seq but in predictions. miR-19a-3p and miR-106b-5p were tested by qRT-PCR from RNA pull-down products (Figures 3C and 3D).

Many lncRNAs, including H19, participate in molecular regulation pathways through their interactions with proteins and modulation of their activities.[23] Combined with the results of RNA pull-down and bioinformatics prediction, PCBP1 and FUS may be the target proteins of H19. PCBP1 is an essential regulator in some cancers. Several findings revealed that PCPB1 might play an important role in preventing the process of epithelial-mesenchymal transition (EMT) in non-small-cell lung cancer, so it might be a promising therapeutic target to inhibit non-small-cell lung cancer (NSCLC)

Figure 5. The Targeted Inhibition of miR-19a-3p and miR-106b-5p Could Decrease the Malignant Progression of CML Cells

(A) K562 cells were transfected with SCR, t-antimiR-19a-3p, and t-antimiR-106b-5p, respectively, and the viability of cells was determined by MTT assay (**$p < 0.01$,*$p < 0.05$, t-antimiR-19a-3p and t-antimiR-106b-5p groups versus BLANK group and SCR group). (B) Inhibition of miR-19a-3p and miR-106b-5p decreases colony formation of K562 cells. A total of 1,000 K562 cells transfected with SCR, t-antimiR-19a-3p, and t-antimiR-106b-5p, respectively, were mixed with RPMI-1640 medium containing 0.9% methylcellulose solution and 20% FBS and seeded into 24-well plates. Colony numbers were reckoned after 1 week. Histogram and statistics indicating the relative number of colonies per 1,000 plated cells are shown. Statistical significance was assessed by one-way ANOVA (*$p < 0.05$, K562, SCR versus t-antimiR-19a-3p and t-antimiR-106b-5p). (C) K562 cells were co-transfected with H19 lentivirus and miR-19a-3p mimics. The viability of cells was determined by MTT assay. (D) K562 cells were co-transfected with H19 lentivirus and miR-106b-5p mimics. The viability of cells was determined by MTT assay.

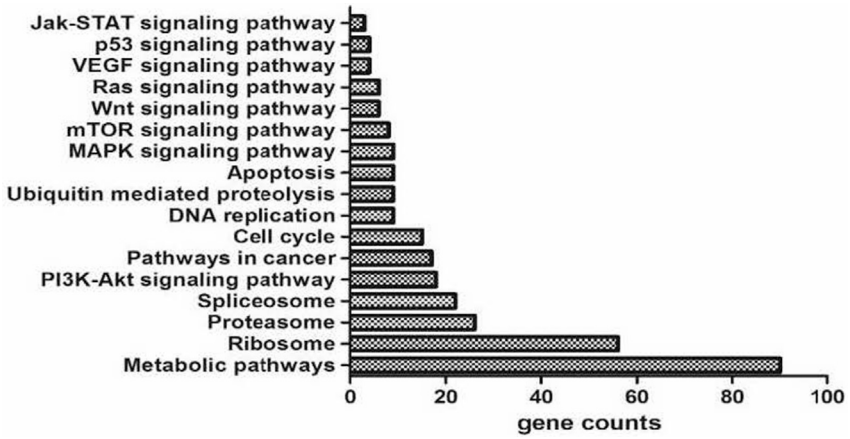

Figure 7. Signal Pathway by Integration of the Signal Molecules from RNA Pull-Down Products by KEGG
Jak-STAT, Ras, and VEGF signaling pathways involved in the H19 RNA pull-down products.

metastasis;[24] PCBP1 might be a prognostic marker for gall bladder carcinoma (GBC) metastasis.[25] Recently, research showed that FUS is a critical gene in some kinds of leukemia, and FUS-ERG protein was identified in acute lymphoblastic leukemia (ALL) and AML.[26] Drug resistance progresses in a large proportion of CML patients and is the main prevention to prolonging survival. IM resistance frequently results from a secondary mutation in BCR-ABL that interferes with drug binding. So the basis of such BCR-ABL-independent IM resistance remains to be explained.[27,28] We showed that targeted inhibition of PCPB1 and FUS enhance the resistance to IM and attenuates the colony-forming ability of K562 cells (Figures 4B and 4C). Co-expression of H19 and PCPB1 (FUS) in K562 cells reverse the inhibitory effect of H19, which reveal the results that the effect of H19 by targeting PCBP1 and FUS proteins.

It has been shown that lncRNAs may act as endogenous sponge RNAs to interact with miRNAs and influence the expression of miRNA target genes. A recent report showed that a muscle-specific lncRNA, linc-MD1, governs the time of muscle differentiation by acting as a competing endogenous RNA in mouse and human myoblasts.[29] lncRNA H19 can also act as a sponge to interact with miR-106a-5p in melanoma cells.[30] The miRNA therapeutics, including inhibition of oncogenic miRNAs or acceleration of tumor-suppressive miRNAs, has been suggested in a large number of studies. For instance, antisense miRNAs can sequester the miRNA competing with target mRNAs by leading to functional inhibition of the certain miRNAs. Antisense-mediated miRNA inhibition can increase binding affinity and improve efficiency *in vivo* by optimizing the oligonucleotides. A variety of chemical modifications achieve this. In our study, we used LNA in which the furanose ring in the sugar-phosphate backbone is chemically locked in an RNA mimicking N-type (C3′ endo) conformation by a 2′-O, 4′-C methylene bridge, into an antisense sequence significantly improve its affinity for the target.[31,32] The targeted inhibition of miR-19a-3p and miR-106b-5p using t-anti-miR-19a-3p and t-anti-miR-106b-5p decrease the cell viability and colony-forming ability of K562 cells and CML patients' bone marrow mononuclear cells (Figures 5A and 5B). Co-expression of H19 and miR19a-3p (miR106b-5p) in K562 cells reverses the inhibition effect of H19; it reveals the results that the effect of H19 by sponging miR19a-3p and miR106b-5p.

We integrated the signaling pathway after RNA pull-down (Figure 7). Many signaling pathways are involved in the progress of CML. For instance, recently, study suggested that the JAK/STAT pathway plays an extremely important role on Dasatinib-induced apoptosis for CML cell model K562.[33] There was a study that indicated that overexpression COX-2 caused upregulation in imatinib-resistant K562 cells through the Wnt and MEK signaling pathway.[34]

In conclusion, this study identifies H19 downexpression in CML. Overexpression of H19 in K562 cells and CML patients' bone marrow mononuclear cells significantly inhibits the cell growth and colony-formation ability. PCBP1, FUS, miRNA-106b-5p, and miRNA-19a-3p are included both in the bioinformatics prediction and RNA pull-down products, which may be the target of H19. Inhibition of the expression of PCBP1 and FUS by siRNA and LNA-modified anti-miRNA-106b-5p and anti-miRNA-19a-3p inhibits cell growth and colony-formation ability. H19 might provide a new treatment strategy for CML.

MATERIALS AND METHODS

Patient Samples, Human Cells, and Cell Lines

Healthy peripheral blood or CML bone marrow samples were obtained from healthy adult donors in Guangdong Provincial Emergency Hospital/the Guangdong Second Provincial General Hospital after written informed consent was obtained according to the institutional guidelines and the Declaration of Helsinki principles. CML bone marrow cells and human peripheral blood mononuclear cells were cultured in 100 ng/mL stem cell factor (SCF), 100 ng/mL granulocyte-colony stimulating factor (G-CSF), 20 ng/mL FMS-like tyrosine kinase 3 (FLT3), 20 ng/mL interleukin (IL)-3, and 20 ng/mL IL-6.

The K562 cells were cultured in RPMI-1640 medium (Gibco, USA) supplemented with 10% fetal bovine serum, 100 IU/mL penicillin, and 100 IU/mL streptomycin. The cells were incubated at 37°C in a humidified atmosphere with 5% CO_2. The medium was changed every 2 days; all cellular assays were conducted in the exponential phase of growth. The K562 cell was purchased from the Institute of Shanghai Cell Biology (Chinese Academy of Sciences, Shanghai, China).

Cell Transfection

The full-length human H19 sequence was synthesized and subcloned into the pEZ-Lv201 vector (GeneCopoeia, Guangzhou, China). K562 cells stably overexpressing H19 or control were established by

transfecting K562 cells with H19-expressing vector (H19 pEZ-Lv201) or empty vector (pEZ-Lv201). Transfection of cells was performed using Lipofectamine 3000 reagent (Invitrogen, USA) following the manufacturer's protocol. The cells were selected in medium containing puromycin (1 mg/mL). The expression of H19 was monitored by real-time PCR assays.

Lentiviral Transduction in CML Patients' Bone Marrow Cells

For the packaging of lentivirus, H19 overexpression plasmids were transfected into HEK293T cells along with the envelope plasmid pCMV-VSVG and packaging plasmid pCMV-dR8.2 using Lipofectamine 2000 (Life Technologies, USA). At 48 h post-infection, the culture media containing lentivirus were collected and CML patients' bone marrow cells (1×106 cells/mL) were infected by spinoculation ($1{,}500 \times g$, 90 min, 32°C) with virus-containing supernatants twice. Cells were harvested 48 h later.

Colony-Forming Assays

The colony assays for dispersed single cells were performed to measure the capacity of cell-colony formation. After the harvest of transfected cells, cells (1×10^3) were mixed completely with RPMI-1640 medium containing 0.9% methylcellulose solution, 20% fetal bovine serum (FBS), 2 mM L-glutamine, and 5 μM 2-mercaptoethanol and seeded onto 24-well plates. Single cells were randomly and evenly distributed throughout the wells. Colonies were formed and counted 2 weeks later using an inverted microscope (Olympus, Japan). The number of colonies containing more than 50 cells was counted. All analysis were performed in triplicate.

Xenograft Mouse Model of Human CML

BALB/c nude mice were used for leukemogenesis experiments and maintained in a temperature and humidity-controlled environment. A total of 500,000 P210 cells transfected with H19 or empty vector were injected into sublethally irradiated (3 Gy) BALB/c recipient mice subcutaneously (seven mice per group). Tumor growth was assessed and tumor sizes were measured every day.

CML Progression in NOD/SCID Mice

In the CML progression assay, the H19-transfected K562 cells were injected into 5-week-old, sublethally irradiated (3 Gy) NOD/SCID recipient mice randomly via tail vein (1×10^7 cells per mouse, seven mice per group). Tumor burden of mice after cell injection was shown by *in vivo* imaging systems.

Establishment of Patient-Derived Xenografts

CML patients' bone marrow cells were transfected with H19 overexpression lentivirus, and then cells (1×10^6 cells/mouse) were transplanted by tail vein injection into sublethally irradiated (300 cGy) 8-week-old NOD/SCID mice. The live time of mice (seven mice per group) were measured.

Polymerase Chain Reaction Assays

The DNA fragment of H19 was PCR-amplified using a T7-containing primer (Sangon Biotech, Shanghai, China) and the high-fidelity DNA polymerase (Thermo Fisher Scientific, USA) on a Bio-Rad C1000 thermal cycler. The following PCR primers were used: H19+T7, F, 5′-TAA TAC GAC TCA CTA TAG GGA GAG GAC CAT GGC CCC G-3′; R, 5′-TTG CTG TAA CAG TGT TTA TTG ATG ATG AGT CCA GGG CTC C-3′. The purification of DNA was performed by agarose gel electrophoresis followed by gel extraction using a gel extraction kit (GBCBIO Technologies, Guangzhou, China).

Transcription *In Vitro* and RNA Pull-Down Assays

The purified DNA was transcribed *in vitro* into RNA by a MEGAscript kit (Thermo Scientific, USA). The 3′ terminus of the RNA strand was attached to a single biotinylated nucleotide by T4 RNA ligase (Pierce RNA 3′ end dethiobiotinlation kit; Thermo Fisher Scientific, USA). Biotinylated RNA (50 pmol) was mixed with washed streptavidin magnetic beads and incubated at room temperature for 30 min with agitation. Cell lysis buffer (protein concentration was greater than 2 mg/mL) was added to the RNA-bound beads, and further incubated for 60 min at 4°C with agitation. The elution buffer was added to the washed RNA-binding protein complexes and mixed well by vortexing. The complexes were incubated for 30 min at 37°C with agitation.

MS

The lncRNA protein-binding complexes from RNA pull-down were detected by MS followed by electrophoresis and Coomassie brilliant blue staining. The catRAPID and starBase v. 2.0 predicted the targeted proteins of lncRNA H19. Specific proteins from RNA pull-down products both existed in MS and prediction were tested by western blot.

Western Blot Analysis

Cells were collected and washed twice with PBS; the Radioimmunoprecipitation assay buffer (RIPA buffer) in the presence of proteinase inhibitor (Selleck Chemicals, Houston, TX, USA) was added. The crude lysates were transferred to pre-chilled Eppendorf tubes and centrifuged at $12{,}000 \times g$ for 15 min at 4°C. The whole-cell lysates were resolved on a 10% SDS-polyacrylamide gel and electrophoretically transferred to PVDF (poluvinlidene difluoride) membrane (Millipore). The membrane was incubated with antibody against PCBP1 (1:1,000, ab168377, Abcam, USA) and β-actin (1:2,000, Santa Cruz Biotech, Santa Cruz, CA, USA) at 4°C overnight. After being washed, these membranes were followed by HRP (horseradish peroxidase)-labeled goat anti-rabbit immunoglobulin G (IgG) (1:2,000, Santa Cruz Biotechnology, USA) at room temperature for 2 h. The signals were visualized with enhanced chemiluminescence (ECL; Beyotime Company) and analyzed using a BI-2000 system. To quantify the protein band intensities, the films were analyzed using NIH ImageJ software.

miRNA First-Strand Synthesis and qRT-PCR Assay

To validate the miR-19a-3p and miR-106b-5p detected by RNA-seq from RNA pull-down products, cDNA was synthesized using poly(A) polymerase (Takara, Japan), and the expression level of miR-19a-3p and miR-106b-5p was determined using SYBR qRT-PCR (Takara,

Japan). miR-19a-3p was amplified with the primer 5′-CTGTGCAA ATCTATGCAAAACTG-3′. miR-106b-5p was amplified with the primer 5′-TAAAGTGCTGACAGTGCAGAT-3′.

siRNAs or t-Anti-miRNA LNAs and Their Transfection

The sequences used in this study were as follows: PCBP1 siRNA (5′-AAGGCGGGTGTAAGA TCAA-3′) and FUS-siRNA (5′-GGAC AGCAGCAAA GCTATA-3′). The RNA duplexes were synthesized and purified by the Guangzhou RiboBio. The sequence of t-anti-miR-19a-3p and t-anti-miR-106b-5p LNAs were designed according to the principle of sequences complementary to seeds of mature miR-19a-3p and miR-106b-5p. The LNA-modified nucleotide sequences used in this study are listed as follows: t-anti-miR-106b-5p (5′-TAAAGTGC-3′); t-anti-miR-19a-3p (5′-TGTGC AAA-3′). The LNA-modified nucleotides were chemically synthesized and modified with LNA by Shanghai Sangon Bio-engineering and stored at −20°C. ALL RNA duplexes were transfected into CML cells using Lipofectamine 2000 according to the manufacturer's instructions.

Cell Viability Assay

Cell viability was determined by MTT assays. In brief, K562 cells were seeded at a density of 1×10^5 cells/mL in 96-well plates (50 μL/well). The cells were transfected with H19 siRNA (100 nM) using Lipofectamine 2000 reagent (Invitrogen, USA) following the manufacturer's protocol. After 6 h, the cells were treated with IM at a concentration of 0.05, 0.1, 0.15, 0.2, 0.25, or 0.3 μmol/L. At 48 h post-treatment, 20 μL MTT stock solution (5 mg/mL) was added to each well, and the plate was incubated for 4 h at 37°C. The media was then removed, and dimenthyl sulfoxide (DMSO) (150 μL) was added to dissolved the blue formazan crystals produced by live cells. Cell viability was assessed by measuring the absorbance at 570 nm on a Bio-Rad microtiter plate reader.

RNA Isolation, Reverse Transcription, and Real-Time PCR Assays

To measure PCBP1 and FUS mRNA expression, total RNA was extracted from K562 cell using Trizol (Invitrogen). After reverse transcription, the levels of PCPB1 and FUS mRNA were determined using a SYBR green real-time PCR assay. The PCR primers used were 5′-CA CCTCTAGATGCCTACTCGATTCAAG-3′ and 5′-ACTGTTGTCT TGCCACCTGGTTC-3′ (PCPB1); 5′-CGGACAGCAGAGTTACAG TGGTTATAG-3′ and 5′-TTGACTGAGTTCCATAGCCTGTGT TC-3′ (FUS); and 5′-CAACGGATTTGGTCGTATT-3′ and 5′-CAC AGTCTTCTGGGTGGC-3′ (GAPAH).

The levels of PCBP1 and FUS mRNA were normalized to that of (glyceraldehyde-3-phosphate dehydrogenase) GAPDH, and the fold-change was calculated using the $2^{-\Delta\Delta CT}$ method.

Statistical Analysis

The data are expressed as means ± standard deviation (SD) of a minimum of three biological replicates. Statistical analysis was carried out by using Microsoft Excel and GraphPad Prism Software v. 6.01 (Systat Software, San Jose, CA, USA). Student's two-tailed unpaired t test was used to determine the significance, and p values < 0.05 were considered statistically significant. The log rank test was used to determine the significant differences of the survival data, and p values < 0.05 were considered statistically significant.

AUTHOR CONTRIBUTIONS

J.F. conceived of and designed the experiments. J.Y., Z.Y., Y. Liu, Y. Li, G.H., and C.G. performed the experiments. J.Y., Z.Y., Y.L., G.H., and C.G. analyzed the data. Z.Y. and Y.L. contributed reagents, materials, and analytical tools. J.F., J.Y., and Z.Y. wrote the paper.

CONFLICTS OF INTEREST

The authors declare no competing interests.

ACKNOWLEDGMENTS

This work was supported by grants from the National Natural Science Foundation of China (no. 81170496), the Research Project for Practice Development of National TCM Clinical Research Bases (no. JDZX2015119), the Science and Technology Program of Guangdong Province (no. 2016A020226027, 2017B030303001), the Science and Technology Program of Guangzhou City (no. 201604020140), the Fundamental Research Funds for the Central Universities (no. 21617461), and the Sanming Project of Medicine in Shenzhen (SZSM201601062).

REFERENCES

1. Apperley, J.F. (2015). Chronic myeloid leukaemia. Lancet *385*, 1447–1459.
2. Huang, X., Cortes, J., and Kantarjian, H. (2012). Estimations of the increasing prevalence and plateau prevalence of chronic myeloid leukemia in the era of tyrosine kinase inhibitor therapy. Cancer *118*, 3123–3127.
3. Fatica, A., and Bozzoni, I. (2014). Long non-coding RNAs: new players in cell differentiation and development. Nat. Rev. Genet. *15*, 7–21.
4. St Laurent, G., Wahlestedt, C., and Kapranov, P. (2015). The Landscape of long noncoding RNA classification. Trends Genet. *31*, 239–251.
5. Yang, Z., Li, X., Yang, Y., He, Z., Qu, X., and Zhang, Y. (2016). Long noncoding RNAs in the progression, metastasis, and prognosis of osteosarcoma. Cell Death Dis. *7*, e2389.
6. Bouckenheimer, J., Assou, S., Riquier, S., Hou, C., Philippe, N., Sansac, C., Lavabre-Bertrand, T., Commes, T., Lemaître, J.M., Boureux, A., and De Vos, J. (2016). Long non-coding RNAs in human early embryonic development and their potential in ART. Hum. Reprod. Update *23*, 19–40.
7. Geng, H., and Tan, X.D. (2016). Functional diversity of long non-coding RNAs in immune regulation. Genes Dis. *3*, 72–81.
8. Zhou, X., Liu, S., Cai, G., Kong, L., Zhang, T., Ren, Y., Wu, Y., Mei, M., Zhang, L., and Wang, X. (2015). Long Non Coding RNA MALAT1 Promotes Tumor Growth and Metastasis by inducing Epithelial-Mesenchymal Transition in Oral Squamous Cell Carcinoma. Sci. Rep. *5*, 15972.
9. Engemann, S., Strödicke, M., Paulsen, M., Franck, O., Reinhardt, R., Lane, N., Reik, W., and Walter, J. (2000). Sequence and functional comparison in the Beckwith-Wiedemann region: implications for a novel imprinting centre and extended imprinting. Hum. Mol. Genet. *9*, 2691–2706.
10. Gabory, A., Jammes, H., and Dandolo, L. (2010). The H19 locus: role of an imprinted non-coding RNA in growth and development. BioEssays *32*, 473–480.
11. Gabory, A., Ripoche, M.A., Yoshimizu, T., and Dandolo, L. (2006). The H19 gene: regulation and function of a non-coding RNA. Cytogenet. Genome Res. *113*, 188–193.

12. Steinhoff, C., Paulsen, M., Kielbasa, S., Walter, J., and Vingron, M. (2009). Expression profile and transcription factor binding site exploration of imprinted genes in human and mouse. BMC Genomics *10*, 144.

13. Li, S., Yu, Z., Chen, S.S., Li, F., Lei, C.Y., Chen, X.X., Bao, J.M., Luo, Y., Lin, G.Z., Pang, S.Y., and Tan, W.L. (2015). The YAP1 oncogene contributes to bladder cancer cell proliferation and migration by regulating the H19 long noncoding RNA. Urol. Oncol *33*, 427.e41–427.e10.

14. Han, D., Gao, X., Wang, M., Qiao, Y., Xu, Y., Yang, J., Dong, N., He, J., Sun, Q., Lv, G., et al. (2016). Long noncoding RNA H19 indicates a poor prognosis of colorectal cancer and promotes tumor growth by recruiting and binding to eIF4A3. Oncotarget *7*, 22159–22173.

15. Zhang, E.B., Han, L., Yin, D.D., Kong, R., De, W., and Chen, J. (2014). c-Myc-induced, long, noncoding H19 affects cell proliferation and predicts a poor prognosis in patients with gastric cancer. Med. Oncol. *31*, 914.

16. Huang, C., Cao, L., Qiu, L., Dai, X., Ma, L., Zhou, Y., Li, H., Gao, M., Li, W., Zhang, Q., et al. (2015). Upregulation of H19 promotes invasion and induces epithelial-to-mesenchymal transition in esophageal cancer. Oncol. Lett. *10*, 291–296.

17. Zhou, J.D., Lin, J., Zhang, T.J., Ma, J.C., Li, X.X., Wen, X.M., Guo, H., Xu, Z.J., Deng, Z.Q., Zhang, W., and Qian, J. (2018). Hypomethylation-mediated H19 overexpression increases the risk of disease evolution through the association with BCR-ABL transcript in chronic myeloid leukemia. J. Cell. Physiol. *233*, 2444–2450.

18. Wahid, F., Shehzad, A., Khan, T., and Kim, Y.Y. (2010). MicroRNAs: synthesis, mechanism, function, and recent clinical trials. Biochim. Biophys. Acta *1803*, 1231–1243.

19. Ameres, S.L., Martinez, J., and Schroeder, R. (2007). Molecular basis for target RNA recognition and cleavage by human RISC. Cell *130*, 101–112.

20. Tessema, M., Länger, F., Bock, O., Seltsam, A., Metzig, K., Hasemeier, B., Kreipe, H., and Lehmann, U. (2005). Down-regulation of the IGF-2/H19 locus during normal and malignant hematopoiesis is independent of the imprinting pattern. Int. J. Oncol. *26*, 499–507.

21. Hao, Y., Crenshaw, T., Moulton, T., Newcomb, E., and Tycko, B. (1993). Tumour-suppressor activity of H19 RNA. Nature *365*, 764–767.

22. Lin, J., Ma, J.C., Yang, J., Yin, J.Y., Chen, X.X., Guo, H., Wen, X.M., Zhang, T.J., Qian, W., Qian, J., and Deng, Z.Q. (2018). Arresting of miR-186 and releasing of H19 by DDX43 facilitate tumorigenesis and CML progression. Oncogene *37*, 2432–2443.

23. Marchese, F.P., Raimondi, I., and Huarte, M. (2017). The multidimensional mechanisms of long noncoding RNA function. Genome Biol. *18*, 206.

24. Liu, Y., Gai, L., Liu, J., Cui, Y., Zhang, Y., and Feng, J. (2015). Expression of poly(C)-binding protein 1 (PCBP1) in NSCLC as a negative regulator of EMT and its clinical value. Int. J. Clin. Exp. Pathol. *8*, 7165–7172.

25. Zhang, H.Y., and Dou, K.F. (2014). PCBP1 is an important mediator of TGF-β-induced epithelial to mesenchymal transition in gall bladder cancer cell line GBC-SD. Mol. Biol. Rep. *41*, 5519–5524.

26. Panagopoulos, I., Gorunova, L., Zeller, B., Tierens, A., and Heim, S. (2013). Cryptic FUS-ERG fusion identified by RNA-sequencing in childhood acute myeloid leukemia. Oncol. Rep. *30*, 2587–2592.

27. Hentschel, J., Rubio, I., Eberhart, M., Hipler, C., Schiefner, J., Schubert, K., Loncarevic, I.F., Wittig, U., Baniahmad, A., and von Eggeling, F. (2011). BCR-ABL- and Ras-independent activation of Raf as a novel mechanism of Imatinib resistance in CML. Int. J. Oncol. *39*, 585–591.

28. Mancias, J.D., Wang, X., Gygi, S.P., Harper, J.W., and Kimmelman, A.C. (2014). Quantitative proteomics identifies NCOA4 as the cargo receptor mediating ferritinophagy. Nature *509*, 105–109.

29. Cesana, M., Cacchiarelli, D., Legnini, I., Santini, T., Sthandier, O., Chinappi, M., Tramontano, A., and Bozzoni, I. (2011). A long noncoding RNA controls muscle differentiation by functioning as a competing endogenous RNA. Cell *147*, 358–369.

30. Luan, W., Zhou, Z., Ni, X., Xia, Y., Wang, J., Yan, Y., and Xu, B. (2018). Long noncoding RNA H19 promotes glucose metabolism and cell growth in malignant melanoma via miR-106a-5p/E2F3 axis. J. Cancer Res. Clin. Oncol. *144*, 531–542.

31. Staedel, C., Varon, C., Nguyen, P.H., Vialet, B., Chambonnier, L., Rousseau, B., Soubeyran, I., Evrard, S., Couillaud, F., and Darfeuille, F. (2015). Inhibition of Gastric Tumor Cell Growth Using Seed-targeting LNA as Specific, Long-lasting MicroRNA Inhibitors. Mol. Ther. Nucleic Acids *4*, e246.

32. Vester, B., and Wengel, J. (2004). LNA (locked nucleic acid): high-affinity targeting of complementary RNA and DNA. Biochemistry *43*, 13233–13241.

33. Dalgıç, C.T., Kaymaz, B.T., Özkan, M.C., Dalmızrak, A., Şahin, F., and Saydam, G. (2015). Investigating the Role of JAK/STAT Pathway on Dasatinib-Induced Apoptosis for CML Cell Model K562. Clin. Lymphoma Myeloma Leuk. *15* (*Suppl*), S161–S166.

34. Dharmapuri, G., Doneti, R., Philip, G.H., and Kalle, A.M. (2015). Celecoxib sensitizes imatinib-resistant K562 cells to imatinib by inhibiting MRP1-5, ABCA2 and ABCG2 transporters via Wnt and Ras signaling pathways. Leuk. Res. *39*, 696–701.